

See discussions, stats, and author profiles for this publication at: <https://www.researchgate.net/publication/228484044>

Time-Resolved EPR Study of the Primary Donor Triplet in D1-D2-cyt b559 Complexes of Photosystem II: Temperature Dependence of Spin-Lattice Relaxation

ARTICLE *in* THE JOURNAL OF PHYSICAL CHEMISTRY · FEBRUARY 1996

Impact Factor: 2.78 · DOI: 10.1021/jp951334r

CITATIONS

26

READS

14

4 AUTHORS, INCLUDING:



Ivan Proskuryakov

Russian Academy of Sciences

41 PUBLICATIONS 304 CITATIONS

SEE PROFILE

Time-Resolved EPR Study of the Primary Donor Triplet in D1-D2-cyt *b559* Complexes of Photosystem II: Temperature Dependence of Spin–Lattice Relaxation

Martin K. Bosch,[†] Ivan I. Proskuryakov,[‡] Peter Gast,[†] and Arnold J. Hoff*,[†]

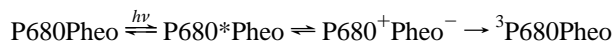
Department of Biophysics, Huygens Laboratory, Leiden University, P.O. Box 9504, 2300 RA Leiden, The Netherlands, and Institute of Soil Science and Photosynthesis, Russian Academy of Sciences, 142292 Pushchino, Moscow Region, Russia

Received: May 12, 1995; In Final Form: October 26, 1995[®]

The temperature dependence of the EPR spectrum and kinetics of the primary donor triplet state ³P680 are measured with direct-detection CW EPR and electron spin echo (ESE) spectroscopy, respectively. The EPR spectrum was recorded up to 230 K; kinetics could be traced up to 70 K. The observed anisotropy of the temperature dependence of the EPR spectrum recorded within 1 μs after a laser flash is explained by anisotropic spin relaxation in the precursor primary radical pair. The ESE-detected decay kinetics of the Z-canonical peak of ³P680 is close to its optical lifetime for *T* < 20 K but deviates strongly from the lifetime for *T* > 30 K, due to a rapid acceleration of spin relaxation with temperature. This relaxation is not caused by the presence of oxygen or the paramagnetic heme iron in the *b559* cytochrome; it is attributed to slow triplet hopping in the P680 dimer itself. Comparison of the low-temperature kinetics with that of chlorophyll *a* in solution confirmed that the central Mg ion in the triplet-bearing Chl of ³P680 is pentacoordinated.

1. Introduction

Photosystem II (PS II) of plants and cyanobacteria is responsible for light-induced water oxidation, accompanied by oxygen evolution. Studies of PS II photochemistry have intensified with the isolation of a relatively simple pigment–protein complex, which preserves certain functional properties of the PS II reaction center (RC).^{1–3} This preparation is known as the D1-D2-cytochrome *b559* complex, and contains 6 chlorophyll (Chl) *a* and 2 pheophytin *a* (Pheo) molecules, 1 or 2 β-carotenes, 1 cytochrome *b559*, and no plastoquinones.^{3–5} Upon illumination the reaction scheme in those particles is as follows:



in which P680 is the primary electron donor and Pheo the primary acceptor. The triplet state of P680 is populated through recombination of the primary radical pair [³(P680⁺Pheo[−])], because electron transport past Pheo is blocked. In contrast, in more intact preparations of PS II, further electron transport involves two quinone molecules, which accept the unpaired electron from Pheo[−].

The PS II reaction center (RC) is thought to be similar in many respects to the much better known RCs of photosynthetic purple bacteria.^{6,7} A number of spectroscopic properties of the PS II RC, however, preclude a straightforward analogy. One example is the EPR observation of the electron-spin-polarized triplet state of the primary donor, ³P. In RCs of *Rb. sphaeroides*, ³P870 can be detected with flash-EPR up to room temperature.⁸ In another purple bacterium, *Rps. viridis*, the triplet spectrum was followed up to 100 K.^{9,10} In contrast, in PS II, EPR of ³P680 was first reported to be detectable only below 6 K.^{11–15} In more recent works, ³P680 could be followed up to 20 K¹⁶ and 30 K.¹⁷ Yet, with optical time-resolved spectroscopy ³P680 was observed up to room temperature with a yield that decreased from 80 to 30% when the temperature was increased from 4 K

to room temperature.^{18–20} The lifetime of ³P680 determined in the optical investigations was of the order of 1 ms for all temperatures. Therefore, the reported absence of the ³P680 EPR signal for *T* > 30 K cannot be explained by a drop in its yield or lifetime.

Population of the spin-polarized triplet of the primary donor molecule when secondary electron transfer is blocked is regarded as a general property of photosynthetic RCs.^{21,22} Thus, the lack of its detection in PS II RCs at elevated temperatures poses questions concerning the mechanism of primary photoprocesses in these RCs and has prompted us to investigate the temperature dependence of the EPR spectrum of ³P680 in more detail. A major difference between optical and EPR measurements of a triplet state is that the signal intensity in the latter case is influenced by spin–lattice relaxation (SLR) properties. Thus, the rapid disappearance of the electron-spin-polarized steady-state EPR spectrum of ³P680 with rising temperature could be the result of such a spin-relaxation process, if the relaxation is faster than the physical lifetime of the triplet. Under such circumstances, time-resolved EPR measurements are advantageous over steady-state ones. Indeed, preliminary data (I. Proskuryakov, unpublished results) demonstrated the feasibility of ³P680 EPR detection up to 90 K, using time-resolved CW EPR. In the present work we have undertaken a more detailed study of ³P680 utilizing two types of magnetic resonance techniques with high time resolution, i.e., electron spin echo (ESE) and direct-detection flash-EPR spectroscopy. The results reported here confirm that the spin relaxation is the main cause for the loss of the ³P680 signal when recorded with the conventional CW EPR technique. When detecting within a microsecond after the exciting light flash, it is possible to observe this signal up to 230 K. In the course of this work we learned of a similar investigation,²³ which for temperatures below 40 K globally corroborates our results.

2. Materials and Methods

D1-D2-cyt *b559* complexes were prepared according to ref 3. The maximum of the red absorption band at room temperature was at 676 nm. The optical density of the preparation

[†] Leiden University. E-mail Hoff@rulhl1.LeidenUniv.nl.

[‡] Russian Academy of Sciences.

[®] Abstract published in *Advance ACS Abstracts*, January 15, 1996.

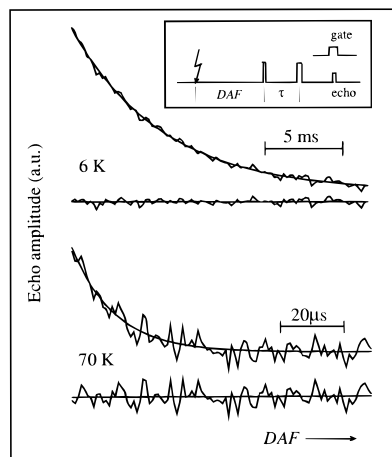


Figure 1. ESE-detected kinetics of $^3\text{P680}$ as observed at the low-field canonical Z-peak at 6 K and 70 K. $\tau = \tau_{\text{max}} = 300$ ns; microwave frequency 9.321 GHz; excitation wavelength 570 nm. Smooth curves represent monoexponential fits; the bottom curves are the residuals. Note the different time scales used. Inset: the sequence of light and microwave pulses used in the measurements.

was $\text{OD}_{676} = 22 \text{ cm}^{-1}$. Quinone-depleted (dQ) RCs of *Rb. sphaeroides* R26 were prepared according to refs 24 and 25 and concentrated to $\text{OD}_{800} = 130 \text{ cm}^{-1}$. RC samples for EPR were prepared by the addition of glycerol (60–70% v/v) as cryoprotectant, and freezing in the dark. Under illumination the conventional CW EPR of the plant and bacterial RC samples revealed the well-known electron-spin-polarized spectra of the primary donor triplet states, $^3\text{P680}$ and $^3\text{P870}$, respectively. Partial removal of oxygen from D1-D2-cyt *b559* preparations was achieved by flushing the sample in the EPR tube with Ar, and subsequent incubation under Ar for 5 h in the dark at 4 °C. In some experiments 20 mM dithionite was added. This procedure was performed under Ar to avoid dithionite oxidation by O_2 . Chl *a* was purified²⁶ and dissolved in ethanol in a concentration of 10^{-4} M. Chl samples were degassed by freeze–pump–thaw cycles.

In field-swept time-resolved experiments a home-built X-band homodyne direct-detection CW EPR setup (flash-EPR) was used, equipped with a Varian rectangular TE_{102} optical transmission cavity with $Q \sim 2000$. The EPR signal obtained after the microwave mixer was amplified by two solid-state wide-band video amplifiers (50 dB total gain) and fed into a Stanford Research SR250 boxcar integrator. The sample was excited with 4 ns flashes (~ 20 mJ per flash) from an OPO-C355 optical parametric oscillator, pumped by a Continuum Surelite I Nd:YAG laser, which was operated at a repetition rate of 9.6 Hz. The excitation wavelength was tunable in the range $400 \text{ nm} < \lambda < 700 \text{ nm}$. The boxcar sampling gate of $1 \mu\text{s}$ duration was synchronized with the laser flash and started at zero delay.

For spin-relaxation measurements the same setup was used, now equipped with a low- Q (~ 400) cavity of a similar design, in the ESE configuration described earlier.^{27,28} A 2-pulse (flash–DAF– $\pi/2$ – τ – π – τ –echo) ESE sequence (8 ns $\pi/2$ -pulse) with fixed delay τ was used to detect transient states after a variable delay-after-flash (DAF) between the laser flash and the first microwave pulse (see Figure 1, inset). The resolution of the setup for triplet rise times (limited by the width of the first pulse) is better than 10 ns, as determined from the rise kinetics of the $^3\text{Chl } a$ signal in ethanol solution (not shown).

The delay τ between the two microwave pulses was adjusted for maximum signal (τ_{max}). For the Z-canonical orientation we found $\tau_{\text{max}} = 300$ ns. It was independent of temperature and had the same value in D1-D2-cyt *b559* particles, Chl *a* in solution, and dQ-RCs of *Rb. sphaeroides* R26.

The temperature was set and stabilized by means of a home-built temperature controller, which registered the temperature in the Oxford Instruments ESR 900 flow cryostat with an Au–Fe/chromel thermocouple positioned close to the sample. Absolute temperature was accurate to within 1 K and stable within 0.1 K. The temperature at the sample position was checked using a calibrated carbon resistor supplied by Netherlands Meetinstituut (NMI).

Kinetic data were fitted by exponential decay functions with a Levenberg–Marquardt routine.²⁹ The zero-field splitting (ZFS) parameters $|D|$ and $|E|$ were determined from field-swept EPR spectra using all six canonical magnetic fields. To increase the accuracy in calculating the Z- and Y-canonical fields, the direct-detection field-swept spectra were numerically differentiated.

3. Results

Two types of measurements were carried out to detect the EPR properties of the triplet as a function of temperature. Kinetics of spin relaxation were detected with ESE spectroscopy; information on the spectral shape was obtained with field-swept flash-EPR.

ESE-Detected Kinetics. Relaxation measurements in CW EPR are hampered by the presence of microwave-induced relaxation. This complication, which is especially severe for electron-spin-polarized spectra, is avoided when using ESE spectroscopy. In this technique there is no microwave field present in the period DAF between the photogeneration of the triplet and its detection.

For all samples studied, we limited ourselves to detecting the kinetics at the Z-canonical field, because at the other parts of the spectrum, notably also at the X- and Y-canonical fields, the kinetics is strongly mixed because of spectral overlap due to the large anisotropy of the triplet dipolar interaction (our peak labeling corresponds to $D, E > 0$,³⁰ see Figure 3).

The rise times of the $^3\text{P680}$ signal at the low-field Z-canonical peak at 10, 40, and 70 K were determined with ESE to be 350, 320, and 305 ns, respectively (data not shown).

Figure 1 shows ESE-detected kinetics of the decay of the $^3\text{P680}$ signal at 6 and 70 K. As can be judged from the residuals, the decays are to a good approximation monoexponential. Figure 2 shows Arrhenius plots of the rate constants k , obtained from the monoexponential fits for the different samples studied. It is seen that for *Rb. sphaeroides* R26 dQ-RCs and Chl *a* in solution (Figure 2, panel A) a strong temperature dependence is observed (2 orders of magnitude in the value of k in the range of 6–160 K). For D1-D2-cyt *b559* the temperature dependence is even stronger. The rate constants determined for $T \leq 20$ K are taken to reflect the physical lifetimes of the triplet states, as will be discussed later.

The temperature dependence shown in Figure 2 was fitted with a T^n power law or an exponential function of reciprocal temperature. We limited the fitting procedure to data points that were over threefold faster than the physical lifetime, in order to account only for kinetics governed by T_1 . Figure 2 displays the best fits. As can be seen from the figure, $^3\text{Chl } a$ and $^3\text{P870}$ decay is best described by a power law, with powers of 2.5 and 3.5, respectively. The temperature dependence of $^3\text{P680}$ relaxation corresponds better to an exponential function; here no satisfactory fit could be obtained with a power law.

To investigate the effect of paramagnetic centers in the vicinity of $^3\text{P680}$ on its relaxation properties, we performed analogous experiments on deoxygenated samples, or under reducing conditions (20 mM dithionite), which treatments transform cyt *b559* to a nonparamagnetic state (Figure 2, panel

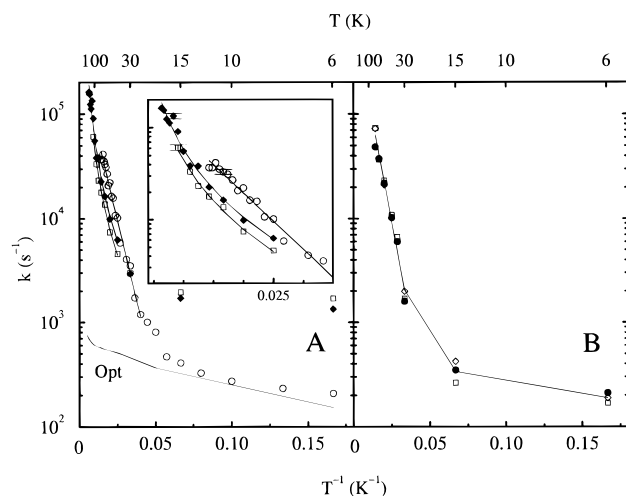


Figure 2. Arrhenius plots of the triplet state EPR signal (low-field Z-peak) decay rates, determined from ESE-detected kinetics as in Figure 1, and of $^3\text{P680}$ lifetime from optical measurements.²⁰ Panel A: $^3\text{P870}$ (open squares); ^3Chl in ethanol (filled diamonds); $^3\text{P680}$ (open circles); optical lifetime of $^3\text{P680}$ (Opt). Solid lines drawn through the data points correspond to the exponential dependence on reciprocal temperature for $^3\text{P680}$ and to a power law for $^3\text{P870}$ and ^3Chl . Inset: expanded view of the high-temperature part of panel A. Error bars were determined from repeated measurements of decay curves. Panel B: temperature dependence of ESE-determined rate constants in nontreated (open squares), O_2^- (open diamonds) and dithionite-containing (filled circles) D1-D2-cyt *b559* samples.

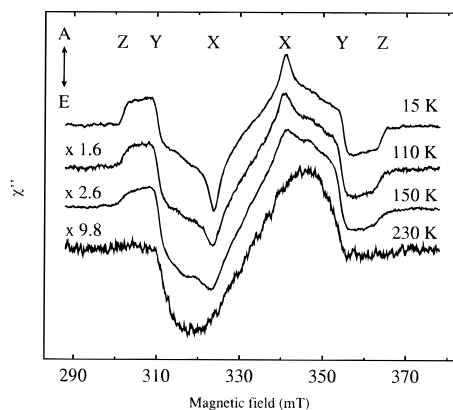


Figure 3. Direct-detection CW flash EPR boxcar spectra of $^3\text{P680}$ in D1-D2-cyt *b559* complexes at different temperatures. Top labels indicate the canonical fields. All spectra are normalized to the 15 K spectrum with the indicated multiplication factors. At 150 and 230 K several accumulations were performed; the 15 and 110 K data were obtained in a single sweep. Experimental conditions: 4 ns flashes at 570 nm; boxcar gate 1 μs , starting at the flash; microwave frequency: 9.341 GHz, sweep time 5 min. A denotes enhanced absorption and E emission of microwaves.

B). No significant changes in k were observed in the whole temperature range compared to nontreated samples. The signal amplitudes in the dithionite-containing sample were measured at 6 K before and after prolonged flash illumination at 100 K. The signal after 30 or 60 min illumination at 100 K decreased 2-fold, compared to the measurement before illumination. For the nontreated D1-D2-cyt *b559* sample, negligible change in signal intensity was observed. The kinetic parameters were not affected by this procedure.

The initial amplitude of the ESE-detected kinetics of $^3\text{P680}$ demonstrates a strong temperature dependence (Figure 4, ESE), which cannot be explained by the drop in the triplet yield, for this yield was reported to decrease only 3-fold in the temperature range studied.²⁰ The most straightforward explanation for such behavior in an ESE experiment is an increase of the spin–spin

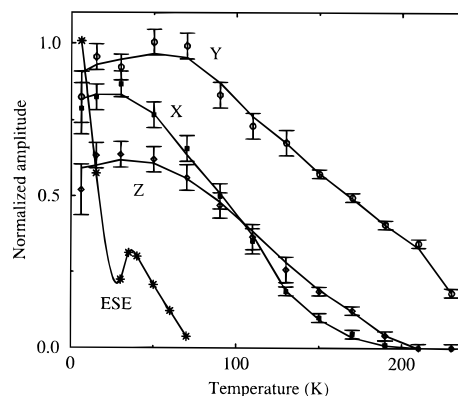


Figure 4. Amplitudes of peaks at the canonical fields (X,Y,Z) taken from the field-swept spectra (Figure 3), as a function of temperature. Trace ESE shows the initial amplitude of the ESE-detected kinetic traces.

relaxation rate (T_2^{-1}) with temperature, so that in the period τ between the two microwave pulses considerable spin dephasing takes place. To verify this, we measured the electron spin echo envelope modulation (ESEEM) curve. At 6 K, modulation could be detected up to 2.5 μs , whereas at 60 K only the first modulation at 300 ns was observed (data not shown). This temperature dependence of T_2 made detection by ESE of the kinetics above ~ 70 K impossible. The nonmonotonous drop in the ESE initial amplitude around $T = 20$ K (Figure 4, ESE) is a reproducible phenomenon and corresponds to an increase of spin–spin relaxation around this temperature. A similar “temperature resonance” was reported for T_1^{-1} of the tyrosyl radical Y_D^\bullet in PS II.²⁷

Field-Swept EPR. Although strong, the observed temperature dependence of the EPR lifetime does not preclude detection of field-swept spectra of $^3\text{P680}$ if the sampling time of the signal is short enough. Since CW-EPR detection is hampered considerably less by spin–spin relaxation effects than ESE, we utilized the direct-detection flash-EPR technique for field-swept measurements. Another advantage of this technique over field-swept ESE is that the latter gives distorted spectra due to differences in the ESEEM modulation pattern observed for different canonical peaks.

Figure 3 presents the flash-EPR spectra of $^3\text{P680}$ in D1-D2-cyt *b559* complexes at several temperatures. The triplet was detected up to 230 K, which is close to the melting point of the sample. The temperature behavior of the canonical peak amplitudes (X,Y,Z) is depicted in Figure 4. With increasing temperature the X-canonical peaks are the first to disappear, around 180 K, followed at higher temperatures ($T > 200$ K) by the Z peaks. We found no detectable signal of $^3\text{Pheo}$ as reported earlier,¹⁷ which most probably is due to the differences in preparations used.

At 6 K, $^3\text{P680}$ spectra were compared for several wavelengths in the tuning range of the laser ($400 \text{ nm} < \lambda < 700 \text{ nm}$). No excitation wavelength dependence of the overall spectral shape (ZFS or polarization) was observed.

When the spectral shape permitted, $|D|$ and $|E|$ values were calculated from the canonical magnetic fields (see Table 1). At low temperature, $|D| = 290 \times 10^{-4} \text{ cm}^{-1}$ and $|E| = 43 \times 10^{-4} \text{ cm}^{-1}$. With increasing temperature the ZFS parameters decrease to $|D| = 284 \times 10^{-4} \text{ cm}^{-1}$ and $|E| = 38 \times 10^{-4} \text{ cm}^{-1}$ at 190 K.

4. Discussion

In the first EPR observations of the triplet state of the primary donor in PS II, the signal could be detected only at very low

TABLE 1: ZFS Parameters at Different Temperatures, Extracted from Flash-EPR Spectra of D1-D2-cyt *b559* Complexes Like Those in Figure 3^a

temp, K	$ D $, $\text{cm}^{-1} \times 10^{-4}$	$ E $, $\text{cm}^{-1} \times 10^{-4}$
6	290 ± 2	43 ± 2
15	290 ± 1	42 ± 1
30	290 ± 1	43 ± 1
90	288 ± 1	42 ± 1
130	287 ± 2	41 ± 2
150	286 ± 2	40 ± 2
170	284 ± 1	40 ± 1
190	284 ± 2	38 ± 2

^a Error limits are estimated from the noise levels.

temperatures ($T < 6$ K).^{11–15,31} An early attempt to measure the temperature dependence of ³P680 field-swept EPR-spectra in D1-D2-cyt *b559* complexes was reported by Searle *et al.*¹⁶ Using CW EPR and continuous illumination of the sample, these authors reported a 2-fold decrease of the ³P680 signal between 5.5 and 10 K and were able to follow the triplet up to 20 K. The decrease in signal intensity on warming was suggested to be due to a temperature-induced change in the triplet population process.

In the present work, using adequate time resolution of the EPR experiment (1 μ s), we were able to detect ³P680 field-swept EPR spectra up to 230 K (Figure 3). With this time resolution, the initial amplitudes of the triplet canonical peaks are shown to change not more than 10% when raising the temperature from 6 to 70 K (Figure 4). Thus, the drop in steady-state EPR amplitude on warming reported by Searle *et al.*¹⁶ cannot be explained by a change of initial triplet population with temperature but should rather be attributed to the different experimental approach adopted by these authors.¹⁶ As will become clear below, the disappearance of the steady-state signals on warming is caused by the strong dependence of the SLR rate (T_1^{-1}) of ³P680 on temperature.

ESE-Detected Kinetics. The ESE-detected decay of the ³P680 signal (Figure 2, panel A) demonstrates a strong temperature dependence. The value of k at 6 K agrees nicely with the CW-EPR results of Searle *et al.*¹⁶ Groot *et al.*²⁰ reported optical measurements of the decay of ³P680 in the temperature range of 6–200 K. For $T < 40$ K these authors observed a biphasic behavior of the decay kinetics, which they attributed to independent depopulation of the ³P680 spin sublevels to the ground state. The slower component was related to depopulation of the z -sublevel and the fast component to depopulation of the x - and y -sublevels, which presumably possess similar depopulation rates. Comparing the temperature dependence of the slow component of Groot *et al.*²⁰ with our data for $T < 20$ K (Figure 2, panel A), we conclude that the ESE-detected kinetics in this low-temperature limit is indeed determined by the physical lifetime of the z -sublevel. For $T > 30$ K the decay is governed by SLR, manifested as a deviation of the ESE-detected decay time from the lifetimes observed in optical experiments. This is the very temperature region where the ³P680 EPR signal was lost in earlier studies.¹⁶ Indeed, the temperature step from 15 to 30 K provokes an over 6-fold increase in relaxation rate, which for steady-state detection will lead to a similar drop in the signal amplitude, bringing it below the detection limit.

At this point it is useful to compare the ³P680 relaxation properties with those of monomeric Chl *a* and *Rb. sphaeroides* R26 dQ-RCs (lacking quinones like D1-D2-cyt *b559*). The curves of k vs T^{-1} , determined for monomeric Chl *a* in solution and *Rb. sphaeroides* R26 dQ-RCs (see Figure 2, panel A), are (accidentally) similar and differ considerably from that of D1-

D2-cyt *b559* complexes. At low temperatures the EPR amplitude of ³P680 decays slower than that of the other triplets, and at ~ 30 K the curves cross and at higher temperatures ³P680 relaxes faster.

The temperature dependence of the decay rate of ³P680 for $T > 30$ K is well described by an exponential function (a straight line in Arrhenius coordinates), whereas the decay rates of ³Chl *a* and ³P870 follow a power law (see Figure 2, panel A, inset). The exponential dependence is a manifestation of a one-phonon thermally-activated (Orbach-type) relaxation, apparently present in ³P680 at temperatures above 30 K, and not operative in ³Chl and ³P870. The straight line in Arrhenius coordinates has a slope corresponding to an activation energy of 97 ± 8 cm^{-1} .

In principle, several mechanisms may account for the fast ³P680 SLR, evidenced by the kinetic data at temperatures above 30 K (Figure 2). With time-resolved optical spectroscopy, Durrant *et al.*¹⁸ observed a large effect of oxygen on the lifetime of ³P680 in D1-D2-cyt *b559* at room temperature. Since oxygen is paramagnetic it may also cause additional SLR in the triplet state, even, as recent EPR results suggest, at low temperature.³² Though the O₂-removal procedure adopted in the present work probably did not result in complete removal of oxygen, we expect at least some changes in the relaxation times in the temperature range studied, if O₂ has indeed an appreciable effect. As the decay of ³P680 is virtually independent of O₂ concentration (Figure 2, panel B), we conclude that interaction with paramagnetic oxygen is not the main reason for the increased SLR at higher temperatures. Another possible relaxer is the paramagnetic iron of oxidized cyt *b559*. The redox state of cytochrome *b559* was assessed by studying the effect of dithionite treatment on ³P680 yield. D1-D2 cyt *b559* complexes with reduced cyt *b559* are capable of low-temperature photo-accumulation of reduced Pheo,^{17,33} inhibiting ³P680 formation. Dithionite treatment of our samples and prolonged illumination at 100 K caused a 50% drop in the triplet yield. In nontreated samples illumination at 100 K practically did not change the triplet yield. These experiments indicate that cyt *b559* is largely oxidized in nontreated samples and is essentially reduced in dithionite-treated samples. As no changes in SLR rate are observed in dithionite-reduced samples compared to nontreated ones (see Figure 2, panel B), we conclude that there is no relaxation effect of paramagnetic cytochrome. One more possible relaxer is non-heme iron. However, as mentioned, this iron atom most probably is lost in the D1-D2-cyt *b559* preparation. From the above survey, we conclude that the strong temperature dependence of SLR at higher temperatures must be an intrinsic property of ³P680.

D1-D2-cyt *b559* complexes demonstrate a weak temperature dependence of $|D|$ and $|E|$ (see Table 1). A much stronger temperature dependence has been reported for the purple bacterium *Rb. sphaeroides*,^{8,9} with $|D|$ growing upon increasing the temperature. In PS I a temperature increase led to a considerable drop in $|E|$ and a minor decrease of $|D|$.³⁴ This behavior has been explained by a thermally activated hopping of the triplet state between pigment molecules of the RC. Such a hopping might account for both the changes in ZFS, and the observed increase of the relaxation rate with temperature. Two extremes may be considered: (a) *fast* hopping (with rate $k_{\text{hopping}} >$ the difference in resonance frequency of the two sites, say $k_{\text{hopping}} > 10\text{--}100$ MHz) or (b) *slow* hopping ($k_{\text{hopping}} < 10\text{--}100$ MHz). A choice between these two hopping models can be made by examining the temperature-dependent changes in ZFS, $|D|$ and $|E|$ of ³P680.

Utilizing the dimeric structural model of P680 put forward in ref 30, with the triplet state at low temperature localized on

a single Chl molecule, and assuming thermally activated fast triplet hopping between the dimer components, it is possible to calculate D and E values of $^3\text{P680}$ at high temperature.³⁵ Starting with the low-temperature values of the ZFS parameters ($D = +290 \times 10^{-4} \text{ cm}^{-1}$ and $E = +43 \times 10^{-4} \text{ cm}^{-1}$; for signs of D and E see refs 30 and 36), we obtain for the high-temperature limit, when the triplet is fully equilibrated between the two Chls, $D = +165 \times 10^{-4} \text{ cm}^{-1}$ and $E = -31 \times 10^{-4} \text{ cm}^{-1}$. Using the experimentally observed change in D , at the highest temperature at which it could be determined (190 K, $D = +284 \times 10^{-4} \text{ cm}^{-1}$) as a conservative first approximation we find that only $(290 - 284)/(290 - 165) = 5\%$ of the higher-energy triplet state is populated. From the observed change in E a similar value may be calculated. Thus, even at 190 K, the triplet is essentially localized on one dimer pigment.

Noguchi *et al.*³⁷ interpreted the temperature dependence of one line in the FTIR spectrum of $^3\text{P680}$ as resulting from hopping of the triplet state between the two dimer components of P680 on a time scale slower than that of Raman excitation ($\sim 10^{-13} \text{ s}$). From this temperature dependence the energy difference ΔE of the two triplet states was determined to be 64 cm^{-1} .³⁷ We estimate that for fast hopping at 190 K the higher-energy triplet should then be populated for 25%. Using our above-determined activation energy (97 cm^{-1}) as an upper limit for ΔE we obtain a lower limit of 16% population of the higher-energy triplet state (fast hopping). Thus, the fast hopping model leads to populations of the higher-energy triplet state that are not compatible with the minor changes in ZFS parameters found in this work, at least in the framework of the spatial organization of the P680 dimer proposed in ref 30.

One argument in favor of fast hopping is that the sudden change in T_2 at about 20 K (Figure 4) might be brought about by a resolved spectral density, associated with fast triplet hopping. A hopping frequency at 20 K of 9 GHz (hopping frequency \sim microwave frequency), however, would correspond to an unrealistic short distance between the two dimer halves. This, and the above considerations, indicate that the fast hopping model does not provide an adequate description of the triplet dynamics.

We now turn to *slow* hopping on a time scale of $\sim 1 \mu\text{s}$. Such slow hopping would not affect the ZFS values appreciably, but it still could provide an effective relaxation channel for $^3\text{P680}$ as a result of the modulation of sublevel spin functions associated with the different orientations of the Chl molecules that constitute the purported P680 dimer.³⁰ Slow hopping between sites with somewhat different ZFS parameters would also account for the observed line broadening in the EPR spectrum at high temperatures (Figure 3).

Slow triplet hopping between molecules with a rotated triplet axes system has been invoked earlier for explaining the Orbach-type temperature dependence of the SLR of the triplet state of aromatic molecules.^{38,39} The small value of the activation energy ($10\text{--}16 \text{ cm}^{-1}$) was interpreted to correspond to the thermally induced population of a higher-lying vibronic state (actually a libration) of the same aromatic molecule. If a similar mechanism were operative in $^3\text{P680}$, then it most probably would be observable for Chl *a* *in vitro* as well, which is not the case (Figure 2). Moreover, the activation energy for the relaxation enhancement we find here (ca. 97 cm^{-1}) is much larger than that found in refs 38 and 39. We therefore favor the model in which the triplet state of P680 is hopping slowly between the two dimer components, which probably are separated by about 11 \AA .^{30,40} Note that the energy gap between the two dimer components ($64\text{--}97 \text{ cm}^{-1}$) is much larger than the small exchange energy anticipated for molecules 11 \AA

apart;⁴¹ it is probably largely due to a nonequivalency of the dimer halves, brought about by a different interaction of the Chls with the protein environment (so-called site splitting).

If $^3\text{P680}$ is actually localized on a single Chl *a* molecule at low temperatures ($T < 20 \text{ K}$), then the difference between the lifetimes detected *in vivo* and those detected *in vitro* (see Figure 2, panel A) should be accounted for. From earlier research it is known that the decay rates of the spin sublevels of $^3\text{Chl } a$ strongly depend on the coordination number of the central Mg ion and is 5-fold smaller in pentacoordinated $^3\text{Chl } a$ than in hexacoordinated $^3\text{Chl } a$.^{42,43} (At 2 K , $k_z = 35 \text{ s}^{-1}$ for pentacoordinated and $k_z = 150 \text{ s}^{-1}$ for hexacoordinated $^3\text{Chl } a$.⁴²) In ethanol, Chl *a* is most probably hexacoordinated at low temperatures.⁴³ In contrast, all Chls in D1-D2-cyt *b559* are reported to be pentacoordinated.^{44–46} The 5-fold longer lifetime observed at low temperatures ($T < 20 \text{ K}$) in D1-D2-cyt *b559* compared to Chl *a* in ethanol therefore confirms the coordination number found earlier for Chl *a* in $^3\text{P680}$. It is noteworthy that in bacterial RCs the same coordination number was posulated from the X-ray structure of *Rps. viridis*,⁴⁷ and verified by Raman spectroscopy,⁴⁸ with both BCHls of the primary donor ligated to histidines. Those histidines are conserved in the protein sequence of the D1 and D2 polypeptides of PS II.⁶

Field-Swept EPR. The CW EPR detection scheme utilized in the present study assures a nondistorted line shape of the triplet EPR spectrum, corresponding to its initial polarization if the detection period is shorter than the SLR. In Figure 3 the spectral shape of $^3\text{P680}$ is shown to change with increasing temperature. Separate canonical components demonstrate different temperature dependences of their initial amplitudes (Figure 4). The temperature dependence of the *Y*-peak initial amplitude agrees nicely with the triplet yield variation reported in ref 20 from optical measurements, indicating that the decrease of the *Y*-peak amplitude with temperature is essentially due to the lower triplet yield. However, the drop in the *Z*- and *X*-peak amplitudes is much stronger (see Figure 4).

Within the framework of the radical pair mechanism of triplet state population,^{21,22} the observed temperature dependence can be explained by anisotropic spin relaxation processes. The disappearance of the *Z*- and *X*-peaks at elevated temperatures can be accounted for by three independent mechanisms. First, the signal amplitude would drop if $^3\text{P680}$ spin relaxation becomes faster than the detection period. Second, the drop might be caused by a decrease in the initial spin polarization of the triplet, if the T_{\pm} sublevels of the precursor radical pair $^3[\text{P680}^+\text{Pheo}^-]$ are populated at higher temperatures. Third, the zero-field decay rates k_x , k_y , k_z may have different temperature dependences. To distinguish between these three mechanisms, we consider the decay kinetics of $^3\text{P680}$. Extrapolation to 200 K of the SLR of the *Z*-peak of $^3\text{P680}$ (Figure 2) results in $k \sim 3 \times 10^5 \text{ s}^{-1}$. Such an acceleration of the decay is not sufficient to cause the disappearance of the *Z*-peaks in the flash-EPR field-swept spectrum at 200 K , detected with a gate width of $1 \mu\text{s}$ (see Figure 3). Neither can this disappearance be attributed to a decrease in triplet yield on warming, because the yield drops only 3-fold over the temperature range $6\text{--}200 \text{ K}$.²⁰

Temperature-induced spectral changes of the ^3P EPR signal similar to those of $^3\text{P680}$ have been reported for *Rps. viridis* RCs, though manifested at lower temperatures.^{9,49,50} One explanation involved coherent $S\text{--}T_{\pm}$ mixing in the radical pair due to a fast relaxing electron spin in the iron–quinone acceptor complex.⁵¹ Direct-detection EPR studies of the temperature dependence of the ^3P spectrum, however, showed that this model

is insufficient to explain the temperature dependence.^{10,52} The decrease of initial polarization was therefore attributed to SLR between the T_0 and T_{\pm} levels of the radical pair, induced by the presence of the high-spin Fe^{2+} ion.¹⁰ A similar mechanism might hold for $^3\text{P680}$, even when the non-heme iron is not a likely candidate (it is most probably absent in D1-D2-cyt *b559* complexes); while other possible relaxers, cyt *b559* and O_2 , did not influence the relaxation of the $^3\text{P680}$ Z-sublevel up to 90 K, relaxation effects on the precursor radical pair cannot be excluded.¹⁰ Thus, the drop in the amplitudes of the X- and Z-peaks on warming might be caused by the decrease of the initial polarization, due to enhanced anisotropic SLR within the precursor radical pair, probably due to dipole-dipole relaxation enhancement (which is strongly anisotropic⁵³).

The third possibility, strong temperature dependence of the zero-field decay rates of $^3\text{P680}$, may also explain the temperature-dependent changes in its EPR spectrum. If k_x and k_z become much faster than k_y at high temperature, then for predominant T_0 population the X- and Z-peaks, but not the Y-peak, would disappear on warming. Work is in progress to distinguish between the latter two mechanisms.

5. Conclusions

It is possible to detect field-swept EPR spectra of $^3\text{P680}$ in D1-D2-cyt *b559* complexes at temperatures up to 230 K, when time-resolved direct-detection CW EPR is utilized with a time resolution $<1 \mu\text{s}$. The spectra thus obtained display an anisotropic temperature dependence of the line shape. This anisotropy is attributed to fast anisotropic SLR in the precursor primary radical pair $^3[\text{P680}^+\text{Pheo}^-]$. A relaxation study utilizing ESE detection showed a rapid buildup of the SLR of $^3\text{P680}$ itself at temperatures above 30 K. Below 20 K the decay is close to the physical lifetime of $^3\text{P680}$. The temperature dependence of the SLR for $T > 30 \text{ K}$ indicates an Orbach-type process characterized by an activation energy of $97 \pm 8 \text{ cm}^{-1}$. We suggest that this thermally activated process is a manifestation of slow hopping of the triplet state (which at low temperature is localized on a single Chl) to the other Chl molecule of the P680 dimer. Such slow hopping also explains the observed small changes in ZFS parameters of P680. The 5-fold longer physical lifetime of $^3\text{P680}$ below 20 K compared to the lifetime of Chl *a* in ethanol confirms that the triplet-bearing Chl in $^3\text{P680}$ is pentacoordinated.

Acknowledgment. We are grateful to S. J. Jansen for isolating the reaction centers and to M. J. Moene for the development of the data-acquisition software. We thank Dr. H. J. van Gorkom for stimulating discussions. This work was supported by the Netherlands Foundation for Chemical Research (SON), financed by the Netherlands Organization for Scientific Research (NWO). I.I.P. acknowledges a travel grant of the Netherlands Organization for Scientific Research (NWO). P.G. is a research fellow of the Royal Netherlands Academy of Arts and Sciences (KNAW).

Nomenclature

BChl = bacteriochlorophyll
 Chl = chlorophyll *a*
 DAF = delay between the laser flash and the first microwave pulse
 dQ = quinone depleted
 EPR = electron paramagnetic resonance
 ESE(EM) = electron spin echo (envelope modulation)
 FTIR = Fourier transform infrared spectroscopy
 P680 = primary donor of photosystem II reaction centers

P870 = primary donor of bacterial reaction centers
 Pheo = pheophytin *a*
 PS II = photosystem II of plants
 RC = reaction center
 SLR = spin-lattice relaxation
 ZFS = zero-field splitting

References and Notes

- (1) Nanba, O.; Satoh, K. *Proc. Natl. Acad. Sci. U.S.A.* **1987**, *84*, 109.
- (2) Chapman, D. J.; Gounaris, K.; Barber, J. *Biochim. Biophys. Acta* **1988**, *933*, 423.
- (3) Van Leeuwen, P. J.; Nieveen, M. C.; Van de Meent, E. J.; Dekker, J. P.; Van Gorkom, H. J. *Photosynth. Res.* **1991**, *28*, 149.
- (4) Kobayashi, M.; Maeda, H.; Watanabe, T.; Nakane, H.; Satoh, K. *FEBS Lett.* **1990**, *260*, 138.
- (5) Gounaris, K.; Chapman, D. J.; Booth, P.; Crystall, B.; Giorgi, L. B.; Klug, D. R.; Porter, G.; Barber, J. *FEBS Lett.* **1990**, *265*, 88.
- (6) Michel, H.; Deisenhofer, J. *Biochemistry* **1988**, *27*, 1.
- (7) Nitschke, W.; Rutherford, A. W. *Trends Biochem. Sci.* **1991**, *16*, 241.
- (8) Hoff, A. J.; Proskuryakov, I. I. *Chem. Phys. Lett.* **1985**, *115*, 303.
- (9) Proskuryakov, I. I.; Shkuropatov, A. Ya.; Voznyak, V. M.; Shuvalov, V. A. *Biofizika* **1988**, *33*, 877.
- (10) Van den Brink, J. S.; Manikowski, H.; Gast, P.; Hoff, A. J. *Biochim. Biophys. Acta* **1994**, *1185*, 177.
- (11) Rutherford, A. W.; Paterson, D. R.; Mullet, J. E. *Biochim. Biophys. Acta* **1981**, *635*, 205.
- (12) Rutherford, A. W.; Mullet, J. E.; Crofts, A. R. *FEBS Lett.* **1981**, *123*, 235.
- (13) Evans, M. C. W.; Atkinson, Y. E.; Ford, R. C. *Biochim. Biophys. Acta* **1985**, *806*, 247.
- (14) Rutherford, A. W. *Biochim. Biophys. Acta* **1985**, *807*, 189.
- (15) Telfer, A.; Barber, J.; Evans, M. C. W. *FEBS Lett.* **1988**, *232*, 209.
- (16) Searle, G. F. W.; Telfer, A.; Barber, J.; Schaafsma, T. J. *Biochim. Biophys. Acta* **1990**, *1016*, 235.
- (17) Frank, H. A.; Hansson, Ö.; Mathis, P. *Photosynth. Res.* **1989**, *20*, 279.
- (18) Durrant, J. R.; Giorgi, L. B.; Barber, J.; Klug, D. R.; Porter, G. *Biochim. Biophys. Acta* **1990**, *1017*, 167.
- (19) Yruela, I.; Van Kan, P. J. M.; Muller, M. G.; Holtzwarth, A. R. *FEBS Lett.* **1994**, *339*, 25.
- (20) Groot, M. L.; Peterman, E. J. G.; Van Kan, P. J. M.; Van Stokkum, I. H. M.; Dekker, J. P.; Van Grondelle, R. *Biophys. J.* **1994**, *67*, 318.
- (21) Hoff, A. J. In *Light Emission by Plants and Bacteria*; Govindjee; Ames, J., Fork, D. C., Eds.; Academic Press, Inc.: Orlando, FL, 1986; p 225.
- (22) Budil, D. E.; Thurnauer, M. C. *Biochim. Biophys. Acta* **1991**, *1057*, 1.
- (23) Van Kan, P. J. M.; Svensson, B.; Van Stokkum, I. H. M.; Styring, S. In *ESF Workshop on Electron and Energy Transfer Dynamics in Photosynthesis and Model Systems, Program and Abstracts*; Jyväskylä, 1994; p 23.
- (24) Feher, G.; Okamura, M. Y. In *The Photosynthetic Bacteria*; Clayton, R. K.; Sistrom, W. R., Eds.; Plenum Press: New York, 1978; p 349.
- (25) Okamura, M. Y.; Isaacson, R. A.; Feher, G. *Proc. Natl. Acad. Sci. U.S.A.* **1975**, *72*, 3491.
- (26) Strain, H. H.; Svec, W. A. In *The Chlorophylls*; Vernon, L. P., Seely, G. L., Eds.; Academic Press: New York, 1966; p 21.
- (27) Evelo, R. G.; Styring, S.; Rutherford, A. W.; Hoff, A. J. *Biochim. Biophys. Acta* **1989**, *973*, 428.
- (28) Evelo, R. G. Ph.D. Thesis, Leiden University, The Netherlands, 1991.
- (29) Press, W. H.; Teukolsky, S. A.; Vetterling, W. T.; Flannery, B. P. *Numerical Recipes in C*, 2nd ed.; Cambridge University Press: Cambridge, U.K., 1992.
- (30) Bosch, M. K.; Proskuryakov, I. I.; Gast, P.; Hoff, A. J. *J. Phys. Chem.* **1995**, *99*, 15310.
- (31) Okamura, M. Y.; Satoh, K.; Isaacson, R. A.; Feher, G. In *Progress in Photosynthesis Research*; Biggins, J., Ed.; Martinus Nijhoff Publishers: Dordrecht, 1987; Vol. 1, p 379.
- (32) Van Kan, P. J. M.; Stokkum, I. H. M.; Styring, S. In *ESF Workshop on the D1/D2/Cyt b559 Complex of PSII, Program and Abstracts*; 1995; p 21.
- (33) Shuvalov, V. A.; Heber, U.; Schreiber, U. *FEBS Lett.* **1989**, *258*, 27.
- (34) Sieckmann, I.; Brettel, K.; Bock, C.; Van der Est, A.; Stehlik, D. *Biochemistry* **1993**, *32*, 4842.
- (35) Hoff, A. J. In *Triplet State ODMR Spectroscopy: Techniques and Applications to Biophysical Systems*; Clarke, R. H., Ed.; Wiley-Interscience: New York, 1982; p 367.
- (36) Thurnauer, M. C. *Rev. Chem. Intermed.* **1979**, *3*, 197.
- (37) Noguchi, T.; Inoue, Y.; Satoh, K. *Biochemistry* **1993**, *32*, 7186.

- (38) Verbeek, P. J. F.; Van 't Hof, C. A.; Schmidt, J. *Chem. Phys. Lett.* **1977**, *51*, 41.
- (39) Verbeek, P. J. F.; Dicker, A. I. M.; Schmidt, J. *Chem. Phys. Lett.* **1978**, *56*, 45.
- (40) Svensson, B.; Van Kan, P. J. M.; Styring, S. In *Proceedings of the Xth International Congress on Photosynthesis, Montpellier*; Mathis, P., Ed.; Kluwer Academic: Dordrecht, in press.
- (41) Molin, Yu. N.; Salikhov, K. M.; Zamaraev, K. I. *Spin Exchange: Principles and Applications in Chemistry and Biology*; Springer-Verlag: Berlin, 1980.
- (42) Clarke, R. H.; Hotchandani, S.; Jagannathan, S. P.; Leblanc, R. M. *Chem. Phys. Lett.* **1982**, *89*, 37.
- (43) Muring, K.; Renge, I.; Sarv, P.; Avarmaa, R. *Spectrochim. Acta* **1987**, *43A*, 507.
- (44) Koyama, Y.; Umamoto, Y.; Akamatsu, A.; Uehara, K.; Tanaka, M. *J. Mol. Struct.* **1986**, *146*, 273.
- (45) Fujiwara, M.; Hayashi, H.; Tasumi, M.; Kanaji, M.; Koyama, Y.; Satoh, K. *Chem. Lett.* **1987**, 2005.
- (46) Ghanotakis, D. F.; De Paula, J. C.; Demetriou, D. M.; Bowlby, N. R.; Petersen, J.; Babcock, G. T.; Yocum, C. F. *Biochim. Biophys. Acta* **1989**, *974*, 44.
- (47) Deisenhofer, J.; Epp, O.; Miki, K.; Huber, R.; Michel, H. *Nature (London)* **1985**, *318*, 618.
- (48) Zhou, Q.; Robert, B.; Lutz, M. In *Progress in Photosynthetic Research*; Biggins, J., Ed.; Martinus Nijhoff: Dordrecht, 1987; Vol. 1, p 395.
- (49) Van Wijk, F. G. H.; Gast, P.; Schaafsma, T. J. *Photobiochem. Photobiophys.* **1986**, *11*, 95.
- (50) Van Wijk, F. G. H.; Gast, P.; Schaafsma, T. J. *FEBS Lett.* **1986**, *206*, 238.
- (51) Hore, P. J.; Hunter, D. A.; Van Wijk, F. G. H.; Schaafsma, T. J.; Hoff, A. J. *Biochim. Biophys. Acta* **1988**, *936*, 249.
- (52) Orlinskii, D. B.; Proskuryakov, I. I. *Biofizika* **1989**, *34*, 324.
- (53) Evelo, R. G.; Hoff, A. J. *J. Magn. Res.* **1992**, *95*, 495.

JP951334R